BIOCHEMISTRY
including biophysical chemistry & molecular biology

Article

pubs.acs.org/biochemistry

Structure of MurNAc 6-Phosphate Hydrolase (MurQ) from *Haemophilus influenzae* with a Bound Inhibitor

Timin Hadi,[†,‡] Saugata Hazra,[†,‡] Martin E. Tanner,*[,§] and John S. Blanchard*[,‡]

[‡]Department of Biochemistry, Albert Einstein College of Medicine, 1300 Morris Park Avenue, Bronx, New York 10461, United States
[§]Department of Chemistry, University of British Columbia, Vancouver, British Columbia V6T 1Z1, Canada

Supporting Information

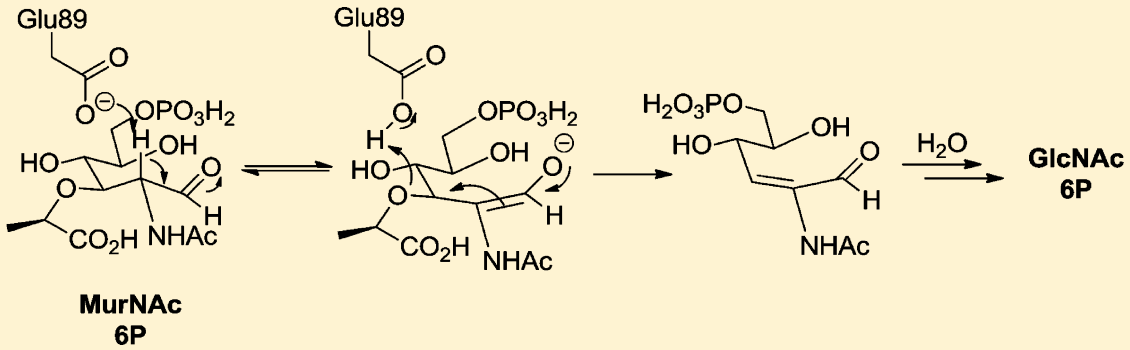

ABSTRACT: The breakdown and recycling of peptidoglycan, an essential polymeric cell structure, occur in a number of bacterial species. A key enzyme in the recycling pathway of one of the components of the peptidoglycan layer, *N*-acetylmuramic acid (MurNAc), is MurNAc 6-phosphate hydrolase (MurQ). This enzyme catalyzes the cofactor-independent cleavage of a relatively nonlabile ether bond and presents an interesting target for mechanistic studies. Open chain product and substrate analogues were synthesized and tested as competitive inhibitors (K_{is} values of 1.1 ± 0.3 and 0.23 ± 0.02 mM, respectively) of the MurNAc 6P hydrolase from *Escherichia coli* (MurQ-EC). To identify the roles of active site residues that are important for catalysis, the substrate analogue was cocrystallized with the MurNAc 6P hydrolase from *Haemophilus influenzae* (MurQ-HI) that was amenable to crystallographic studies. The cocrystal structure of MurQ-HI with the substrate analogue showed that Glu89 was located in the proximity of both the C2 atom and the oxygen at the C3 position of the bound inhibitor and that no other potential acid/base residue that could act as an active site acid/base was located in the vicinity. The conserved residues Glu120 and Lys239 were found within hydrogen bonding distance of the C5 hydroxyl group and C6 phosphate group, suggesting that they play a role in substrate binding and ring opening. Combining these results with previous biochemical data, we propose a one-base mechanism of action in which Glu89 functions to both deprotonate at the C2 position and assist in the departure of the lactyl ether at the C3 position. This same residue would serve to deprotonate the incoming water and reprotonate the enolate in the second half of the catalytic cycle.

Peptidoglycan is an essential portion of the bacterial cell wall in both Gram-positive and Gram-negative bacteria.[1] This polymeric structure functions as a physical barrier from the environment and is important in preventing lysis caused by the strong osmotic pressure exerted upon the cell. The structure of peptidoglycan is comprised of alternating *N*-acetylglucosamine (GlcNAc) and *N*-acetylmuramic acid (MurNAc) monosaccharides linked together via β-(1→4) glycosidic linkages. Amino acids are attached to the D-lactyl ether moiety at the C3 position of the MurNAc residues, and it is through these amino acids that cross-links are formed between neighboring strands to create the three-dimensional structure that surrounds the bacterial cell. Although the exact composition of the peptidoglycan layer can vary immensely from organism to organism, or under different physiological conditions, for the most part, the repeating disaccharide unit remains the same.[1,2]

Because of its essential nature and the key role that it plays during the bacterial cell life cycle, significant research effort has focused on understanding the biosynthesis and metabolism of peptidoglycan. The metabolism of peptidoglycan via recycling and salvage pathways has been studied in a number of organisms, but perhaps most extensively in the Gram-negative bacterium *Escherichia coli*.[3] A number of more recent studies have examined the fate of the monosaccharide MurNAc in the peptidoglycan recycling pathway in *E. coli*.[4−7] Briefly, the disaccharide unit is first cleaved by the glycosidase NagZ to generate GlcNAc and 1,6-anhydro-*N*-acetylmuramic acid; the anhydro sugar is then converted by the hydrolyzing kinase, AnmK, to generate *N*-acetylmuramic acid 6-phosphate

Received: August 1, 2013
Revised: November 14, 2013
Published: November 19, 2013

dx.doi.org/10.1021/bi4010446 | *Biochemistry* 2013, 52, 9358−9366

(MurNAc 6P), and finally, the D-lactyl ether of MurNAc 6P is cleaved by the MurNAc 6P hydrolase, MurQ, to generate *N*-acetylglucosamine 6-phosphate (GlcNAc 6P), for assimilation in the GlcNAc recycling pathway (Figure 1).

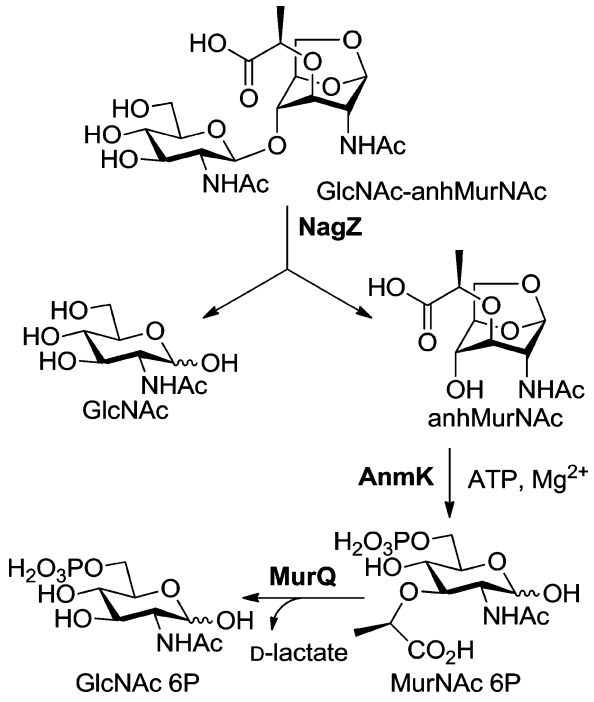

Figure 1. Breakdown of the GlcNAc-anhMurNAc subunit via the peptidoglycan recycling pathway.

The MurQ hydrolase is a particularly interesting target for mechanistic studies as it catalyzes the cleavage of a nonlabile ether bond at the C3 position of MurNAc 6P. Previous work has provided a proposed mechanism of action and helped to identify possible active site residues involved in catalysis (Figure 2).[6,7] A ring opening of MurNAc 6P, likely enzyme-catalyzed, first serves to generate the C1 aldehyde and consequently acidifies the hydrogen at the C2 position. This hydrogen is deprotonated by an active site acid/base residue (B_1) to generate a resonance-stabilized enolate anion. The enolate then undergoes a *syn* elimination of D-lactate, aided by a catalytic acid/base residue (B_2), to generate a Δ2,3-unsaturated (*E*)-alkene intermediate.[7] In a sequence that mirrors the elimination of lactate, B_2 first serves to deprotonate an incoming water molecule for addition at the C3 position of the alkene intermediate to generate the enolate anion. This enolate is then protonated at the C2 position by B_1 to generate the open chain form of GlcNAc 6P. Ring closure then generates the two anomers of the pyranose form of GlcNAc 6P. Experiments using site-directed mutants identified Glu83 and Glu114 as key residues for catalysis and tentatively assigned their roles as B_2 and B_1, respectively, in the proposed mechanism.[7]

MurQ has not been deemed essential in *E. coli*, but there is a dearth of information regarding the enzyme's role in peptidoglycan recycling in other microorganisms.[8,9] Interestingly, recent studies have indicated that homologues in other organisms play a more important role under certain growth conditions.[10] With these considerations in mind, the synthesis and testing of compounds **1** and **2** as potential inhibitors of MurQ from *E. coli* (termed MurQ-EC for the sake of clarity) was undertaken (Figure 2). Compounds **1** and **2** are analogues of GlcNAc 6P and MurNAc 6P, respectively, that are reduced at the C1 position. They were designed to mimic the open chain forms of the product and substrate while lacking the acidic hydrogen at the C2 position that is necessary for MurQ catalysis to occur. These compounds could also serve as useful tools for probing the active site acid/base residues that are important for MurQ catalysis in a cocrystal structure. Although the crystal structure of the *E. coli* enzyme has yet to be determined, a crystal structure of a homologue of MurQ from *Haemophilus influenzae* was previously reported as a part of structural genomics project (previously termed YfeU but reassigned as MurQ and will be termed MurQ-HI in this work).[11] In this study, the cocrystal structure of the enzyme MurQ-HI from *H. influenzae* with compound **2** is reported [Protein Data Bank (PDB) entry 4LZJ]. The activity of the *H. influenzae* MurQ homologue as a MurNAc 6P hydrolase was confirmed, and analysis of the active site acid/base residues surrounding the bound compound **2** was performed. The new information garnered from this structure is used along with previous mechanistic studies to propose a modified mechanism of enzyme action.

EXPERIMENTAL PROCEDURES

Materials and General Methods. MurNAc 6P was prepared in six chemical steps from GlcNAc as described previously.[7] ^{1}H nuclear magnetic resonance (NMR) spectra were recorded on a Bruker DRX300 instrument at a field strength of 300 MHz. Mass spectrometry was performed by electrospray ionization (ESI-MS) using an Esquire LC mass spectrometer in negative mode. Protein concentrations were determined by Bradford analysis using bovine serum albumin as the standard.

Reduced GlcNAc 6P Inhibitor (1). GlcNAc 6P (56 mg, 0.173 mmol) was dissolved in D_2O, and sodium borohydride was added (50 mg, 1.32 mmol). The mixture was then transferred to a NMR tube and heated at 37 °C overnight. The ^{1}H NMR spectrum of the mixture taken after overnight incubation revealed that the peaks corresponding to the anomeric hydrogens of GlcNAc 6P were absent, suggesting that the reduction of the aldehyde at the C1 position was complete. The pH of the reaction mixture was adjusted to 2.0 by the addition of acetic acid and concentrated *in vacuo*. Toluene was added to the residue, and the mixture was concentrated *in vacuo* to remove residual acetic acid. The crude product was dissolved in H_2O and applied to a 5 mL column of AG-1X8 resin (formate form); the resin was then washed successively with 50 mL of H_2O, 50 mL of 1.4 N formic acid, 50 mL of 2.8 N formic acid, and finally 100 mL of 5.6 N formic acid. Each fraction was analyzed by mass spectrometry; those containing compound **1** were pooled, and their volume was reduced *in vacuo*. Distilled water was added to the solution, and the remaining solvent was evaporated; this procedure was repeated multiple times to remove residual formic acid. Compound **1** (37 mg, 0.122 mmol, 70%) was dissolved in H_2O, and the pH of the solution was adjusted to 7.1 with 0.1 N NaOH. The solution was frozen and lyophilized to give the sodium salt of **1** as a white powder: ^{1}H NMR (Figure S1 of the Supporting Information, 300 MHz, D_2O) δ 4.05−3.80 (m, 4H), 3.76−3.37 (m, 4H), 1.95 (s, 3H); ESI-MS *m*/*z* 302.1 $[M - H]^-$.

Reduced MurNAc 6P Inhibitor (2). MurNAc 6P (29 mg, 0.069 mmol) was dissolved in 100 mM deuterated triethanol-

dx.doi.org/10.1021/bi4010446 | *Biochemistry* 2013, 52, 9358−9366

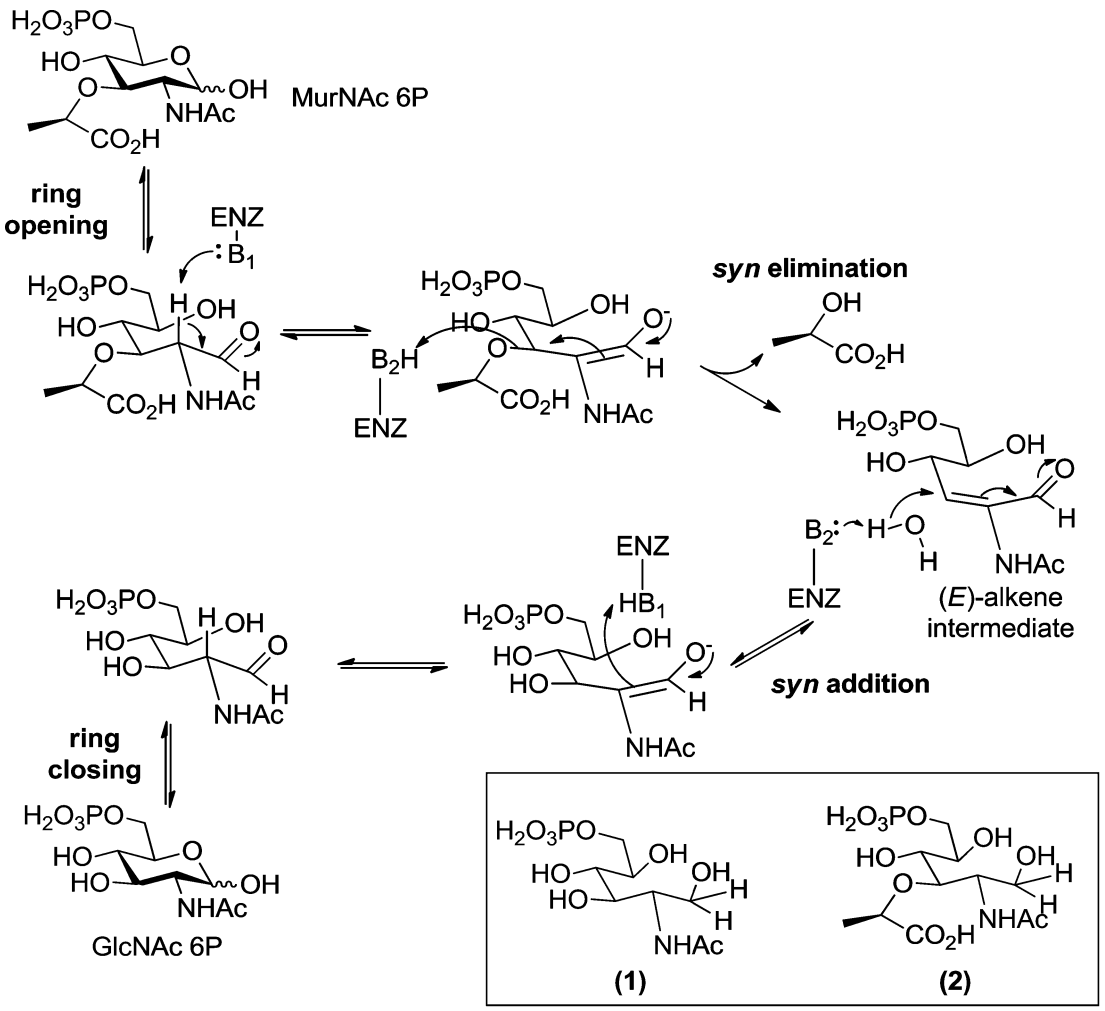

Figure 2. Proposed mechanism of MurNAc 6P hydrolase catalysis and structures of GlcNAc 6P and MurNAc 6P open chain analogues **1** and **2**, respectively (boxed).

amine buffer (pD 8.0), and sodium borohydride (53 mg, 1.40 mmol) was added. The solution was stirred at room temperature for 48 h, and a portion was transferred to a NMR tube for analysis by ^{1}H NMR spectroscopy. The ^{1}H NMR spectrum of the solution revealed that the peaks corresponding to the anomeric hydrogens of MurNAc 6P were absent, suggesting that the reduction of the aldehyde at the C1 position was complete. The reaction mixture was frozen and subsequently lyophilized to give a white powder. The crude product was dissolved in H_2O and applied to a 5 mL column of AG-1X8 resin (formate form); the resin was then washed successively with 100 mL of H_2O, 50 mL of 1.4 N formic acid, 100 mL of 2.8 N formic acid, and finally 100 mL of 5.6 N formic acid. Each fraction was analyzed by mass spectrometry; those containing compound **2** were pooled, and their volume was reduced *in vacuo*. Distilled water was added to the solution, and the remaining solvent was evaporated; this procedure was repeated multiple times to remove residual formic acid. Compound **2** (23 mg, 0.060 mmol, 88%) was dissolved in H_2O, and the pH of the solution was adjusted to 8.3 with 0.1 N NaOH. The solution was frozen and lyophilized to give the sodium salt of compound **2** as a white powder: ^{1}H NMR (Figure S2 of the Supporting Information, 300 MHz, D_2O) δ 4.11−3.95 (m, 2H), 3.91−3.78 (m, 3H), 3.74−3.48 (m, 4H), 1.94 (s, 3H), 1.27 (d, J = 6.8 Hz, 3H); ESI-MS m/z 374.1 $[M - H]^-$.

Cloning, Overexpression, and Purification of *E. coli* MurQ (MurQ-EC) and *H. influenzae* MurQ (MurQ-HI). The wild-type MurQ-EC enzyme from *E. coli* was overexpressed and purified as described previously.[6,7] The enzyme used for kinetic studies was prepared fresh from frozen cell pellets as required because of its reported instability.

The *H. influenzae* MurQ-HI gene (HI0754) was amplified via PCR from *H. influenzae* KW20 Rd genomic DNA as a template using 5′-GGT ATT GAG GGT CGC ATG AAT GAC ATT ATA TTA AA-3′ as the forward primer and 5′-AGA GGA GAG TTA GAG CCT TAT TTA GAA AGC GCA TTT C-3′ as the reverse primer. The underlined sequences are the overhang regions designed for ligation-independent cloning. The PCR product was cloned into the pET-30 Xa/LIC vector (Novagen) according to the manufacturer's protocol. The recombinant plasmid, encoding the MurQ-HI gene product with an N-terminal hexahistidine tag and a Factor Xa cleavage site, was amplified using NovaBlue GigaSingles competent cells (Novagen), and the MurQ-HI gene sequence was subsequently verified.

The recombinant MurQ-HI-containing pET-30 Xa/LIC plasmid was transformed into T7 Express *E. coli* competent cells and plated on LB agar plates containing (30 μg/mL)

dx.doi.org/10.1021/bi4010446 | *Biochemistry* 2013, 52, 9358−9366

kanamycin. The transformed *E. coli* cells were grown overnight at 37 °C while being shaken at 225 rpm in 30 mL of LB medium containing 30 μg/mL kanamycin. This starter culture was used to inoculate 6 L of LB medium containing 30 μg/mL kanamycin, and the resultant mixture was incubated at 37 °C while being shaken at 225 rpm until an A_{600} of 0.6 was reached. Isopropyl β-D-galactopyranoside (IPTG) was added to a final concentration of 0.5 mM, and the cultures were grown for an additional 3.5 h at 37 °C. The cells were harvested by centrifugation at 4000 rpm for 15 min, and the cell pellet was stored at −78 °C. The pelleted cells were resuspended in 70 mL of 50 mM phosphate buffer [500 mM NaCl and 10 mM imidazole (pH 8.0)] containing one tablet of Complete EDTA-free protease inhibitor cocktail and lysed by multiple passes through a cell homogenizer (15000 psi). The lysate was centrifuged at 15000 rpm for 40 min and then poured into 5 mL of Ni-NTA agarose resin. The lysate/resin mixture was mixed for 20 min at 4 °C before being poured into a disposable column. The resin was washed with 50 mM phosphate buffer [500 mM NaCl (pH 8.0)] containing increasing levels of imidazole (10, 50, and 500 mM) in a stepwise fashion. Fractions were analyzed by sodium dodecyl sulfate−polyacrylamide gel electrophoresis (SDS−PAGE), and those containing the MurQ-HI protein were pooled and dialyzed overnight at 4 °C against 4 L of 50 mM Tris buffer [300 mM NaCl (pH 7.5)]. The protein was concentrated using an Amicon 10K MWCO centrifugal device and loaded onto a Hiload 26/60 Superdex 200 preparatory grade gel filtration column. The column was washed with 50 mM Tris buffer [300 mM NaCl (pH 7.5)], and MurQ-HI-containing fractions were pooled and concentrated using an Amicon 10K MWCO centrifugal device. Glycerol was added to the enzyme as a cryoprotectant [20% (v/v)], and the solution was stored at −78 °C.

For crystallographic studies, the N-terminal hexahistidine tag was cleaved using Factor Xa (Novagen) according to the manufacturer's instructions. The cleavage of the protein was monitored by taking aliquots of the cleavage reaction mixture at different time points and analyzing them by SDS−PAGE. The cleaved protein was exchanged into 50 mM Tris buffer [300 mM NaCl (pH 7.5)], and glycerol [20% (v/v)] was added. The MurQ-HI solutions (25 mg/mL) were snap-frozen and stored at −78 °C until they were required for crystallization experiments.

Inhibitor Kinetic Assays. The inhibitory activity of compounds **1** and **2** with respect to the enzymatic activity of MurQ-EC was determined using a coupled spectrophotometric assay monitoring the release of D-lactate as described previously.[7] All kinetic assays were performed at 30 °C in 60 mM triethanolamine-HCl buffer (pH 8.0) containing 0.65 mM *p*-iodonitrotetrazolium violet (INT), 5 mM NAD^+, 10 units of diaphorase, 30 units of D-lactate dehydrogenase, a fixed amount of MurQ-EC, and variable concentrations of MurNAc 6P and either compound **1** or **2** (total volume of 1 mL). MurQ-EC dilutions for kinetic assays were stabilized by the addition of 5% (v/v) of a 10 mg/mL BSA solution in H_2O. Each assay was initiated by the addition of MurNAc 6P after incubation at 30 °C for 10 min. The rate was determined by measuring the change in absorbance at 500 nm due to the reduction of INT. Initial rates were fit to eq 1 for competitive inhibition using Sigmaplot, version 11.0, and the kinetic parameters were determined using this fit.

$$v = (k_{cat}[S])/[K_S(1 + [I]/K_{is})] + [S] \quad (1)$$

Crystallography. Protein crystallization was performed by using the sitting drop vapor diffusion method. The initial MurQ-HI protein sample at 8 mg/mL (200 mM NaCl, 50 mM HEPES, and 5% glycerol) was screened using MCSG crystal screens I−IV. Flat thin crystals were obtained using condition MCSGI-B2 [0.2 M NaCl, 0.1 M Bis-Tris-HCl (pH 5.5), and 25% (w/v) PEG 3350], and thin needle-type crystals appeared from condition MCSGIII-G6 [0.17 M ammonium sulfate, 25.5% (w/v) PEG 4000, and 15% (v/v) glycerol]. Iterated microseeding resulted in efficient crystal growth as well as improved morphology, producing diffraction quality crystals of the protein. Significant improvement was observed for the crystals obtained from the MCSGI-B2 condition, and these were used for future experiments. The crystals were incubated at room temperature (298 K).

Soaking, Data Collection, and Refinement. Crystals of the refined apoproteins appeared after 5 days. Before data were collected, the crystals were flash-frozen in liquid N_2 using mineral oil as a cryoprotectant. Diffraction data were collected from a single frozen crystal using a RAXIS-IV^{++} detector mounted on a Rigaku RH-200 rotating anode (copper anode) X-ray generator. The data were processed using HKL2000.[12] A previously determined structure of MurQ-HI (previously called YfeU, PDB entry 1NRI)[11] was used to phase the data using the CCP4 software suite.[13] Multiple rounds of structural refinement and model building were performed in Refmac5, Phenix,[14−16] and Coot.[17] Structural figures were generated using PyMOL.[18] Atomic coordinates and experimental structure factors have been deposited in the Protein Data Bank (entry 4M0D). The crystals belong to space group $P2_12_12_1$ with the following cell dimensions: a = 76.13 Å, b = 111.65 Å, c = 134.51 Å, and $\alpha = \beta = \gamma = 90.00°$. Table S1 (Supporting Information) lists the other data collection statistics as well as the final refinement statistics for the apo structure.

Diffraction quality MurQ-HI apo crystals were soaked with 50 mM compound **2** in mother liquor. Crystals were flash-frozen after being soaked for 60, 120, and 180 min. Before the crystals were frozen, mineral oil was added to the solution as a cryoprotectant. Diffraction data were collected from a single crystal soaked for 120 min.

Data collection and refinement were performed using the same methods described above. Atomic coordinates and experimental structure factors have been deposited in the Protein Data Bank (entry 4LZJ). Table S2 (Supporting Information) lists the data collection statistics as well as the final refinement statistics for the structure of the MurQ-HI−compound **2** complex.

RESULTS

Testing of Compounds 1 and 2 as Inhibitors of MurQ-EC. Open chain analogues of the product and substrate were expected to serve as inhibitors of the MurQ-catalyzed reaction. Compounds **1** and **2** were synthesized through borohydride reduction of GlcNAc 6P and MurNAc 6P, respectively, and tested as inhibitors of *E. coli* MurQ activity. Both compounds acted as competitive inhibitors of MurQ-EC with K_{is} values of 1.1 ± 0.3 mM (Figure S3 of the Supporting Information) and 0.23 ± 0.02 mM (Figure S4 of the Supporting Information), respectively.

dx.doi.org/10.1021/bi4010446 | *Biochemistry* 2013, 52, 9358−9366

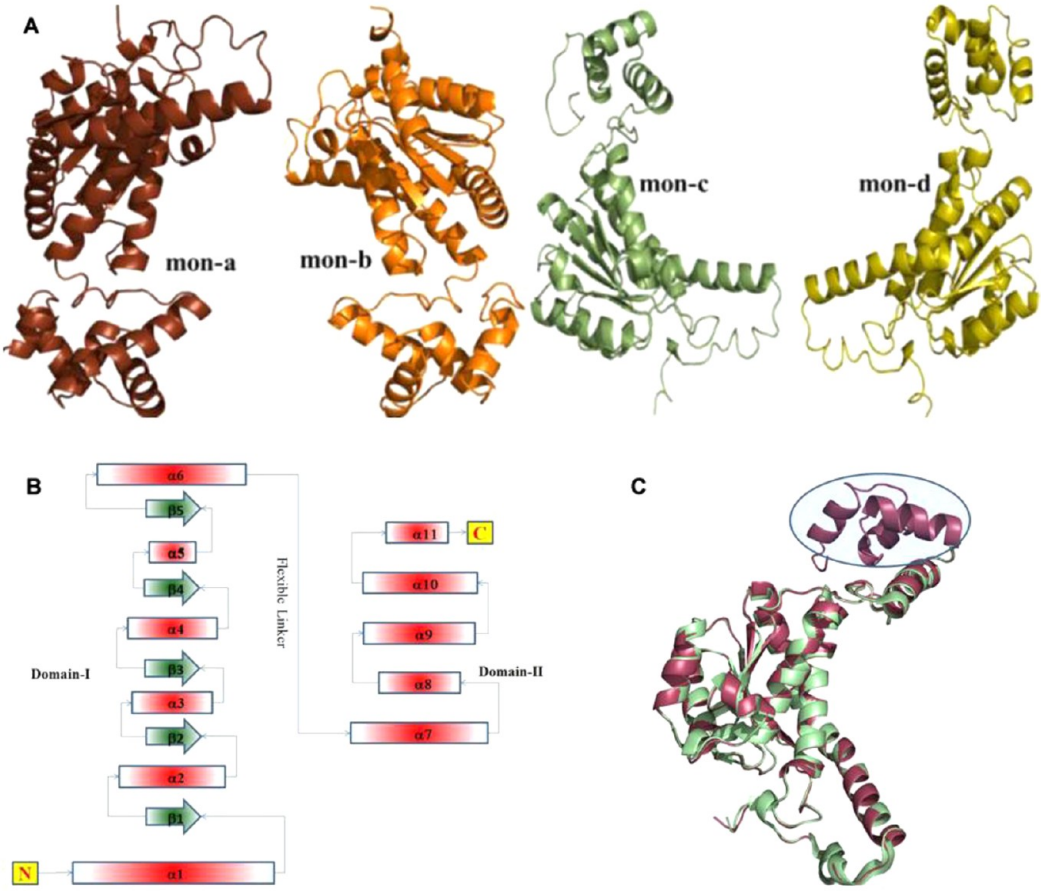

Figure 3. Crystal structure of MurQ-HI. (A) Structure of monomers A–D of MurQ-HI with bound compound **2**. (B) Secondary structure map of the MurQ-HI monomer. (C) Overlay of the MurQ-HI apo monomer (purple) with the previously determined monomer structure (green, PDB entry 1NRI); the previously undetermined region is encircled.

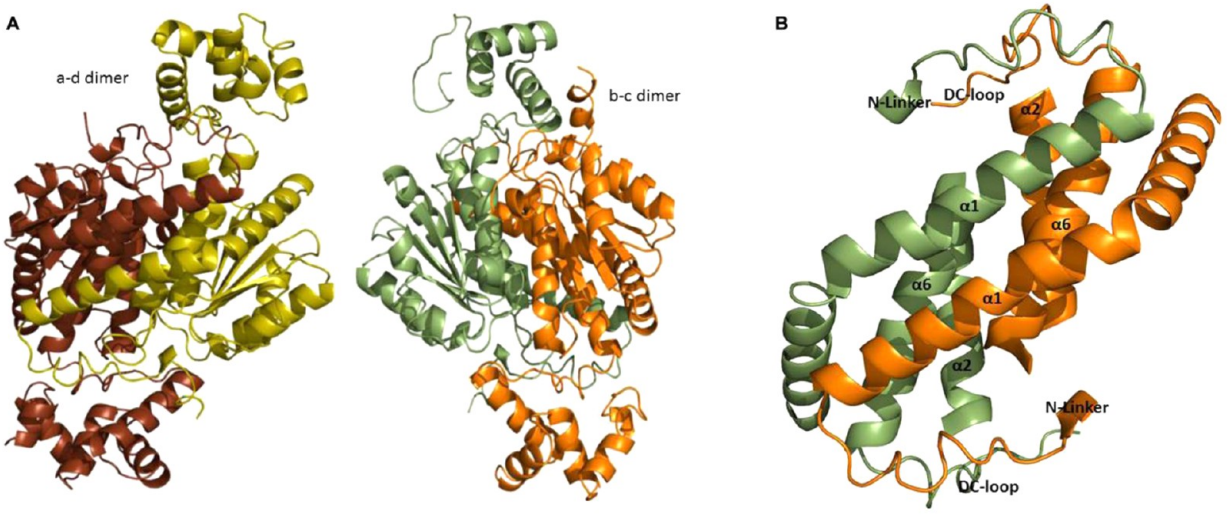

Figure 4. (A) Structure of the MurQ-HI (with bound compound **2**) A–D and B–C dimers. (B) Dimer interface interactions among helices α1, α2, and α6 and N-terminal and domain connector (DC) loops.

Crystallographic Studies of MurQ-HI. The MurQ-HI protein containing a N-terminal hexahistidine tag was overexpressed in *E. coli* and purified. The recombinant protein was incubated with MurNAc 6P and shown to be active as a MurNAc 6P hydrolase (data not shown). Crystals of MurQ-HI were grown and the structure of the apoenzyme was determined to a resolution of 2.6 Å. Crystals of the apoenzyme were then soaked with compound **2** to obtain an enzyme–inhibitor complex. The structure of the complex containing compound **2** was determined to a resolution of 2.4 Å. The structures of the apoenzyme and the enzyme in complex with

dx.doi.org/10.1021/bi4010446 | *Biochemistry* 2013, 52, 9358–9366

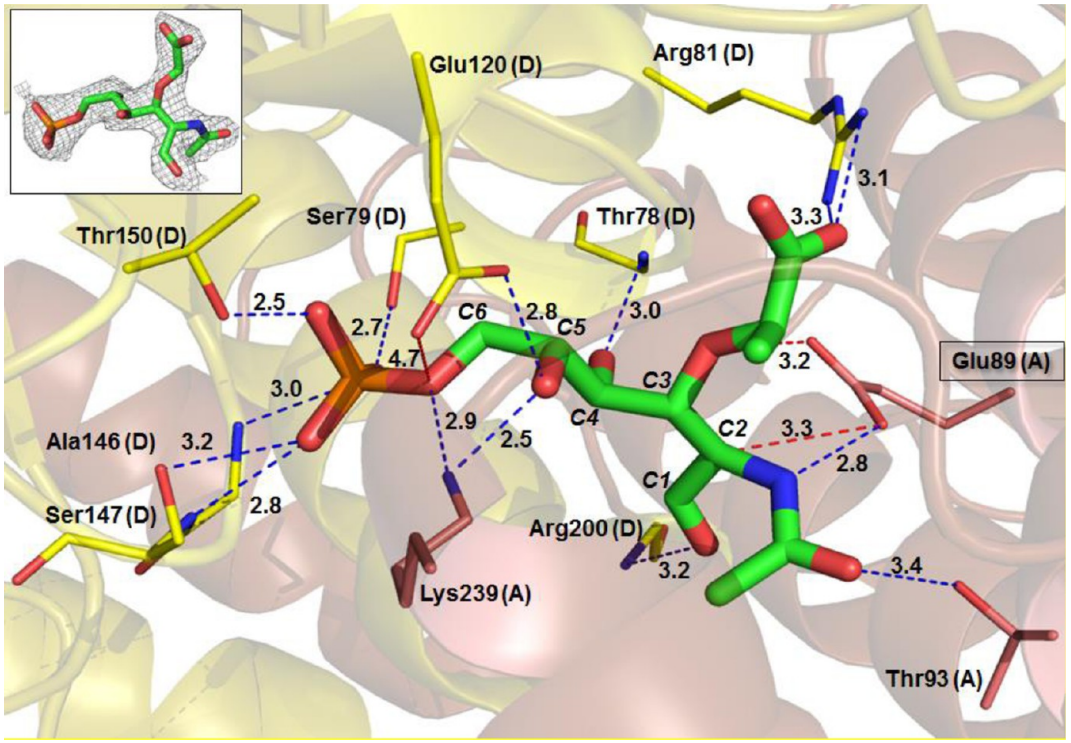

Figure 5. Active site interactions in the MurQ-HI active site (domains A and D) with compound **2** and electron density map of compound **2** (inset).

compound **2** were determined as tetramers by molecular replacement using PDB entry 1NRI as the template.[11]

The MurQ-HI tetramer is composed of four monomers [labeled A–D (Figure 3A)], and each of these monomers is composed of two domains, labeled I and II (Figure 3B). N-Terminal domain I is the larger and more rigid domain and is comprised of six α helices and five β sheets. The five β sheets are surrounded by α helices on both the concave and convex sides. Domain II is comprised of five α helices and is linked to domain I by a long flexible linker (Figure 3B). A portion of domain II was absent in the previously determined apo structure of MurQ-HI; in this study, we present the full length structure of the protein, including this previously undetermined region of domain II (Figure 3C). The overall structure of the monomer is an $\alpha/\beta/\alpha$ sandwich that is analogous to the NAD(P)/FAD-binding Rossmann fold. This domain fold is commonly found in many proteins related to phosphosugar-like isomerases, phosphosugar binding proteins, and regulatory proteins controlling the expression of genes involved in the synthesis of phosphosugars.[19−21]

In both of the determined structures, two dimers are formed, one between monomers A and D and the other between monomers B and C (Figure 4A). The dimers are formed by the head-to-tail interactions between each of the monomers. Five secondary structural constituents play an important role in forming the dimer interface; the interacting components on each monomer are helices α1, α2, and α6 and both the N-terminal and domain connector loop (Figure 4B). The active site is constructed by the contribution of two separate monomers from each of the dimer pairs (A–D and B–C). In the case of the A–D dimer in complex with compound **2**, the active site is formed by Thr93, Gln89, and Lys239 from monomer A, while Thr78, Ser79, Arg81, Glu120, Ala146, Ser147, and Thr150 residues are contributed by monomer D (Figure 5). Additional electron density due to compound **2** is present in the active site (Figure 5, inset), and a number of active site residues are found in the proximity of the inhibitor. The carboxylic acid oxygen of the putative acid/base catalyst Glu89 (monomer A, Glu83 in MurQ-EC) is 3.2 Å from the C3 oxygen and 3.3 Å from C2 of compound **2**. Glu120 (monomer D, Glu114 in MurQ-EC) is 2.8 Å from the C5 oxygen but not in the proximity of either C2 (6.6 Å) or the C3 oxygen (5.1 Å) of compound **2**. The Lys239 (monomer A) ϵ-amino group is 2.5 Å from the C5 oxygen, 2.9 Å from the C6 oxygen, and 3.8 Å from the C6 phosphate oxygen.

DISCUSSION

The results of the inhibitor design and crystallographic studies reported here provide additional insight into the proposed mechanism of action of MurNAc 6P hydrolases outlined in Figure 2. When combined with previous biochemical studies of this class of enzymes,[7] the crystallographic data obtained with bound inhibitors allow for a more definitive assignment of specific roles to important active site acid/base residues involved in catalysis. The synthesis of compounds **1** and **2** represents the first reported attempts at inhibitor design for the MurNAc 6P hydrolase enzyme. These compounds are analogues of the open chain sugars formed as intermediates in the MurQ reaction. They may therefore be expected to bind with greater affinity than the corresponding substrates. It has previously been established that Schiff base formation is not involved in the MurQ reaction, and therefore, reduction of the C1 aldehyde should not dramatically affect binding.[7] Compound **1**, a mimic of the open chain GlcNAc 6P product of the reaction, does not function as a potent inhibitor of MurQ-EC with a K_{is} of 1.1 ± 0.3 mM that is in the same range as the K_M of the MurNAc 6P substrate (1.2 ± 0.1 mM). However, compound **2**, a mimic of the MurNAc 6P substrate of the reaction, is a 5-fold better inhibitor of MurQ-EC with a K_{is} of 0.23 ± 0.02 mM. The fact that the substrate analogue of this

dx.doi.org/10.1021/bi4010446 | *Biochemistry* 2013, 52, 9358−9366

reaction is a more potent inhibitor than the product analogue is not unexpected, and we hypothesize that this is due to the additional binding interactions gained because of the presence of the D-lactyl ether group at the C3 position of compound **2**.

Neither compound **1** nor compound **2** underwent any reaction in the presence of MurQ-EC or MurQ-HI, providing further evidence that a carbonyl is required at the C1 position for catalysis to occur (Figure 2). This lack of reactivity with the enzyme allowed for the potential use of these compounds as active site probes in structural studies. The apo crystal structure of MurQ-HI from *H. influenzae* was previously reported as part of a structural genomics project (PDB entry 1NRI).[11] This protein was predicted to serve the same functional role as MurQ-EC from *E. coli* based on its high degree of sequence identity (55%, *E* value of 2×10^{-95}) and sequence similarity (72%). The coordinates of the MurQ-HI structure, along with those of the homologous enzyme glucosamine 6-phosphate synthase (GlmS), were previously used as the basis of a structural model of MurQ-EC.[7,9] This model was used successfully to identify the catalytically important active site residues Glu83 and Glu114.[7] These observations, along with the reported instability of MurQ-EC,[6] led us to believe that MurQ-HI would be a superior system for studying the structure of inhibitor complexes via X-ray crystallography.

The MurQ-HI complex with compound **2** represents the first crystal structure of a MurNAc 6P hydrolase with a bound inhibitor. A literature search revealed that outside of the previously determined apo structure no structural information is available for proteins with sequences that are more than 35% identical to that of this protein family. Analysis of the cocrystal structure of MurQ-HI with compound **2** allowed for the examination of key contacts in the active site pocket. A multiple-sequence alignment of MurNAc 6P hydrolases revealed that residues Glu89 and Glu120 in MurQ-HI were conserved and were equivalent to Glu83 and Glu114, respectively, in MurQ-EC (see Figure S5 of the Supporting Information for sequence alignment). Glu89 is 3.2 Å from the C3 oxygen atom and 3.3 Å from the C2 atom, placing it in a position to perform the role of either B_1 or B_2 (or both) in the catalytic mechanism.

Previous studies of residues Glu83 and Glu114 in the MurQ-EC enzyme tentatively assigned them as the acid/base residues involved in both the elimination of the D-lactate and subsequent hydration of the (*E*)-alkene intermediate [B_1 and B_2 (Figure 2)].[7] This assignment was attributed to the dramatic decrease in catalytic activity observed upon mutation of either residue. A low rate of solvent-derived deuterium incorporation occurred at the C2 position of unreacted MurNAc 6P when the Glu83Ala reaction was performed in D_2O. Such a deuterium incorporation into residual pools of starting material was not observed when similar incubations were performed with the wild-type enzyme or a Glu114Ala mutant.[7] The incorporation of deuterium suggested that a base (B_1) was still available to deprotonate at the C2 position of the substrate in the Glu83Ala mutant. The lack of incorporation of deuterium into residual pools of starting material with the wild-type enzyme (despite possessing an intact B_1 and B_2) was attributed to the rapid and essentially irreversible elimination of D-lactate following enzyme-catalyzed deprotonation of MurNAc 6P; this elimination was shown to be >10000-fold slower in the Glu83Ala mutant.[7] These observations led to the suggestion that Glu83 may act as B_2 in the MurQ reaction mechanism and, in turn, that Glu114 may play the role of B_1.

Examination of the crystal structure of MurQ-HI with compound **2**, however, is somewhat at odds with these previous assignments. No residue other than Glu89 (corresponding to Glu83 in *E. coli* MurQ) is located within 5.5 Å of the C2 position of the inhibitor. The high degree of structural similarity between compound **2** and the open chain intermediate strongly suggests that Glu89 plays the role of B_1 and acts to deprotonate the C2 position during catalysis. This raises the question of how deuterium exchange can occur with the Glu83Ala mutant of the *E. coli* enzyme. One explanation is that the residues that stabilize the enolate are still present in this mutant and therefore the acidity of the C2 position is still reduced. It may be possible that a surreptitious base in the enzyme active site is able to take the place of Glu83 and catalyze a slow deprotonation at the C2 position. One such possible base is the carboxylate of the lactate side chain that might swing over and transiently occupy the position that is left vacant by the removal of the Glu γ-carboxylate. In this position, it could catalyze the proton transfers that would explain the observed solvent isotope incorporation with the mutant. This notion is consistent with the observation that the Glu83Gln MurQ-EC mutant also shows dramatically impaired catalytic activity yet does not incorporate solvent-derived deuterium. In this case, the Gln side chain sterically impedes the motion of the lactate group (or other surreptitious base) and prevents it from playing such a role. Glu120 (Glu114 in MurQ-EC) was previously identified as an important active site residue in catalysis and a possible candidate for deprotonation as B_1. Examination of the current structure, however, shows that it is 6.6 Å from the C2 position and is unlikely to play a role in deprotonation or protonation at this position. As an alternative to the two-base mechanism outlined in Figure 2, we propose that a single active site residue functions both to deprotonate at the C2 position to generate the resonance-stabilized enolate anion and to assist in the departure of the D-lactate group at the C3 position during catalysis (Figure 6). This same residue would serve to deprotonate the incoming water and reprotonate the enolate in the second half of the catalytic cycle. A candidate for this role is Glu89 (Glu83 in MurQ-EC) as it is located in the proximity of both C2 and C3 of compound **2** in the cocrystal structure with MurQ-HI. We propose that Glu120, positioned within 2.8 Å of the C5

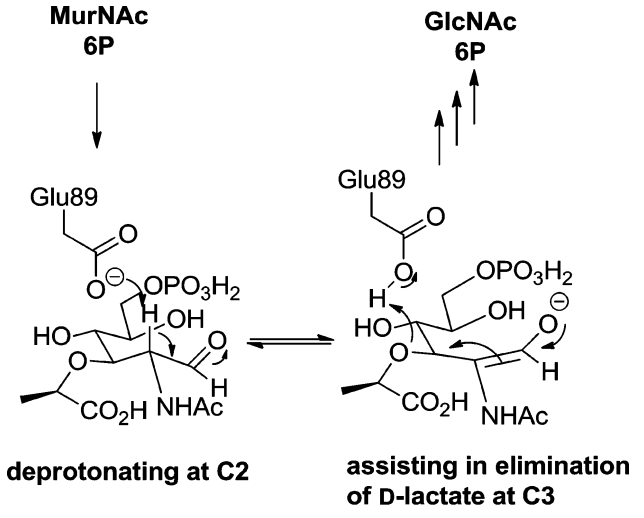

Figure 6. Proposed dual role of Glu89 in MurQ catalysis.

dx.doi.org/10.1021/bi4010446 | *Biochemistry* 2013, 52, 9358−9366

hydroxyl group, does not function as B_1 or B_2 but plays an important role in binding and stabilization of the ring-opened form of the monosaccharide species and possibly in the ring opening and ring closing of the substrate and product of the reaction. The conserved Lys239 residue appears to play a role in binding of the phosphate group at the C6 position or in the stabilization of the ring-opened form of the substrate through an interaction with the C5 hydroxyl group. There are also a number of side chain and backbone hydrogen bonding interactions surrounding the C1 oxygen that could be important in the binding of the carbonyl at the C1 position or the stabilization of the corresponding enolate anion intermediate formed during the course of the enzymatic reaction.

Although compound **2** was not a potent inhibitor of the MurQ-EC enzyme, it served as an excellent active site probe in these crystallographic studies. Analysis of the interactions between compound **2** and the residues in the active site allowed the proposal of a revised mechanism of enzyme action in which Glu89 plays a dual role in catalysis and helped to identify many binding interactions that could be useful for inhibitor design. However, future efforts in synthesizing inhibitors for the MurNAc 6P hydrolases will be largely dependent upon the characterization of the role of peptidoglycan recycling in pathogens other than *E. coli*.

■ ASSOCIATED CONTENT

Supporting Information

^{1}H NMR spectra of compounds **1** and **2**, inhibitor kinetic data with MurQ-EC, multiple-sequence alignment, and crystallographic data tables. This material is available free of charge via the Internet at http://pubs.acs.org.

■ AUTHOR INFORMATION

Corresponding Authors

*Department of Biochemistry, Albert Einstein College of Medicine, 1300 Morris Park Ave., Bronx, NY 10461. Telephone: 718-430-3096. Fax: 718-430-8565. E-mail: john.blanchard@einstein.yu.edu.

*Department of Chemistry, University of British Columbia, Vancouver, British Columbia V6T 1Z1, Canada. Telephone: 604-822-9453. Fax: 604-822-2847. E-mail: mtanner@chem.ubc.ca.

Author Contributions

†Timin Hadi and Saugata Hazra contributed equally to this work.

Funding

This work was supported by National Institutes of Health Grant AI60899 to J.S.B. and a grant from the Natural Sciences and Engineering Research Council of Canada to M.E.T.

Notes

The authors declare no competing financial interest.

■ ACKNOWLEDGMENTS

We thank members of the laboratory of Dr. Steven Almo, particularly Yuriy Patskovsky, Rahul C. Bhosle, and Matthew W. Vetting, for aiding in crystallization efforts.

■ ABBREVIATIONS

anhMurNAc, 1,6-anhydro-*N*-acetylmuramic acid; EDTA, ethylenediaminetetraacetic acid; ESI-MS, electrospray ionization mass spectrometry; FAD, flavin adenine dinucleotide; GlcNAc, *N*-acetylglucosamine; GlcNAc 6P, *N*-acetylglucosamine 6-phosphate; GlmS, glucosamine 6-phosphate synthase; HEPES, 4-(2-hydroxyethyl)piperazine-1-ethanesulfonic acid; INT, *p*-iodonitrotetrazolium violet; IPTG, isopropyl β-D-galactopyranoside; LB, Luria broth; MurNAc, *N*-acetylmuramic acid; MurNAc 6P, *N*-acetylmuramic acid 6-phosphate; MurQ, *N*-acetylmuramic acid 6-phosphate hydrolase; MWCO, molecular weight cutoff; NAD^+, nicotinamide adenine dinucleotide (oxidized form); NADP, nicotinamide adenine dinucleotide phosphate; Ni-NTA, nickel nitriloacetic acid; PCR, polymerase chain reaction; PEG, polyethylene glycol.

■ REFERENCES

(1) Vollmer, W., Blanot, D., and De Pedro, M. A. (2008) Peptidoglycan structure and architecture. *FEMS Microbiol. Rev. 32*, 149−167.

(2) Vollmer, W. (2008) Structural variation in the glycan strands of bacterial peptidoglycan. *FEMS Microbiol. Rev. 32*, 287−306.

(3) Park, J. T., and Uehara, T. (2008) How bacteria consume their own exoskeletons (turnover and recycling of cell wall peptidoglycan). *Microbiol. Mol. Biol. Rev. 72*, 211.

(4) Dahl, U., Jaeger, T., Nguyen, B. T., Sattler, J. M., and Mayer, C. (2004) Identification of a phosphotransferase system of *Escherichia coli* required for growth on *N*-acetylmuramic acid. *J. Bacteriol. 186*, 2385−2392.

(5) Uehara, T., Suefuji, K., Valbuena, N., Meehan, B., Donegan, M., and Park, J. T. (2005) Recycling of the anhydro-*N*-acetylmuramic acid derived from cell wall murein involves a two-step conversion to *N*-acetylglucosamine-phosphate. *J. Bacteriol. 187*, 3643−3649.

(6) Jaeger, T., Arsic, M., and Mayer, C. (2005) Scission of the lactyl ether bond of *N*-acetylmuramic acid by *Escherichia coli* "etherase". *J. Biol. Chem. 280*, 30100−30106.

(7) Hadi, T., Dahl, U., Mayer, C., and Tanner, M. E. (2008) Mechanistic studies on *N*-acetylmuramic acid 6-phosphate hydrolase (MurQ): An etherase involved in peptidoglycan recycling. *Biochemistry 47*, 11547−11558.

(8) Reith, J., and Mayer, C. (2011) Peptidoglycan turnover and recycling in Gram-positive bacteria. *Appl. Microbiol. Biotechnol. 92*, 1−11.

(9) Jaeger, T., and Mayer, C. (2008) *N*-Acetylmuramic acid 6-phosphate lyases (MurNAc etherases): Role in cell wall metabolism, distribution, structure, and mechanism. *Cell. Mol. Life Sci. 65*, 928−939.

(10) Jiang, H., Kong, R., and Xu, X. (2010) The *N*-acetylmuramic acid 6-phosphate etherase gene promotes growth and cell differentiation of cyanobacteria under light-limiting conditions. *J. Bacteriol. 192*, 2239−2245.

(11) Kim, Y., Quartey, P., Ng, R., Zarembinski, T. I., and Joachimiak, A. (2009) Crystal structure of YfeU protein from *Haemophilus influenzae*: A predicted etherase involved in peptidoglycan recycling. *J. Struct. Funct. Genomics 10*, 151−156.

(12) Otwinowski, Z., and Minor, W. (1997) Processing of X-ray diffraction data collected in oscillation mode. *Methods Enzymol. 276*, 307−326.

(13) Potterton, E., Briggs, P., Turkenburg, M., and Dodson, E. (2003) A graphical user interface to the CCP4 program suite. *Acta Crystallogr. D59*, 1131−1137.

(14) Adams, P. D., Afonine, P. V., Bunkoczi, G., Chen, V. B., Davis, I. W., Echols, N., Headd, J. J., Hung, L. W., Kapral, G. J., Grosse-Kunstleve, R. W., McCoy, A. J., Moriarty, N. W., Oeffner, R., Read, R. J., Richardson, D. C., Richardson, J. S., Terwilliger, T. C., and Zwart, P. H. (2010) PHENIX: A comprehensive Python-based system for macromolecular structure solution. *Acta Crystallogr. D66*, 213−221.

(15) Murshudov, G. N., Vagin, A. A., and Dodson, E. J. (1997) Refinement of macromolecular structures by the maximum-likelihood method. *Acta Crystallogr. D53*, 240−255.

(16) Pannu, N. S., Murshudov, G. N., Dodson, E. J., and Read, R. J. (1998) Incorporation of prior phase information strengthens

maximum-likelihood structure refinement. *Acta Crystallogr. D54*, 1285−1294.
(17) Emsley, P., and Cowtan, K. (2004) Coot: Model-building tools for molecular graphics. *Acta Crystallogr. D60*, 2126−2132.
(18) *The PyMOL Molecular Graphics System*, version 1.3r1 (2010) Schrodinger, LLC, Portland, OR.
(19) Sorensen, K. I., and Hove-Jensen, B. (1996) Ribose catabolism of *Escherichia coli*: Characterization of the *rpiB* gene encoding ribose phosphate isomerase B and of the *rpiR* gene, which is involved in regulation of *rpiB* expression. *J. Bacteriol. 178*, 1003−1011.
(20) Peschke, U., Schmidt, H., Zhang, H. Z., and Piepersberg, W. (1995) Molecular characterization of the lincomycin-production gene cluster of *Streptomyces lincolnensis* 78-11. *Mol. Microbiol. 16*, 1137−1156.
(21) Teplyakov, A., Obmolova, G., Badet-Denisot, M. A., and Badet, B. (1999) The mechanism of sugar phosphate isomerization by glucosamine 6-phosphate synthase. *Protein Sci. 8*, 596−602.